

Resonant mode lifetimes due to boundary wave emission in equilateral triangular dielectric cavities

G M Wysin[†]

E-mail: wysin@phys.ksu.edu

Departamento de Física, Universidade Federal de Viçosa, Viçosa, 36570-000, Minas Gerais, Brazil

Abstract. Lifetimes are estimated for the two-dimensional resonant optical modes of a dielectric cavity with an equilateral triangular cross section, that are approximately confined by total internal reflection. Exact solutions of a two-dimensional scalar wave equation for triangular geometry with Dirichlet boundary conditions are used to describe approximately the vector fields of the possible transverse electric (TE) and transverse magnetic (TM) modes. Only two-dimensional electromagnetic solutions are considered here, where there is no propagation vector perpendicular to the plane of the triangle ($k_z = 0$). The field properties just inside and outside the cavity boundary are shown to be significantly different for TE and TM field polarizations, the two cases having different dependences on the index mismatch with the exterior. For a given mode specified by particular quantum numbers, TE polarization leads to longer lifetime than TM polarization at high index mismatch, assuming that escape of evanescent boundary waves at the corners is the primary decay process.

Submitted to: *J. Opt. A: Pure Appl. Opt.*

PACS numbers: 41.20.-q, 42.25.-p, 42.25.Gy, 42.60.-v, 42.60.Da

1. Introduction

Interest continues in micro-lasers and micro-resonators with various geometries, including disks [1], triangles [2, 3], squares [4, 5, 6] and hexagons [7, 8, 9]. Materials with potential device application include various cleaved semiconductor structures [2, 3] and zeolite $\text{ALPO}_4\text{-5}$ crystals [7]. Understanding how geometry controls internal field distributions and hence mode frequencies, lifetimes and associated quality factors (Q) is essential to device development.

Here we consider mode lifetimes in equilateral triangular-based resonator (ETR) cavities confined by total internal reflection (TIR). Triangular geometry mode wavefunctions were reviewed and experimentally measured by Chang *et al.* [2], but

[†] Permanent address: Department of Physics, Kansas State University, Manhattan, KS 66506-2601 U.S.A.

only under the assumptions of TM polarization together with 100% reflectivity of the cavity faces. In a high-index cavity surrounded by a lower index environment, however, the confinement of modes is provided by TIR. Huang *et al.*[10, 11, 12] considered both TE and TM polarizations for dielectric ETRs surrounded by air, using analytic approximations and matching of the interior fields to nonzero exterior fields to estimate mode frequencies. Also, by modeling the response of a cavity to a finite input pulse using a numerical finite difference time domain technique[11, 12], very large Q-factors (1000 – 20000) were estimated for some of the lowest modes, with the highest Q's associated with TM polarization. Considerably lower Q-factors (20 – 150) were measured in GaInAs-InP ETRs with edges from 5 – 20 μm , using the photoluminescence spectrum[3]. Due to the complexity of correctly matching interior oscillatory fields to decaying evanescent exterior fields, simple approximations which may lead to estimates of the mode lifetimes or equivalently, the Q-factors, are considered here.

The evanescent fields in TIR on the outside of the cavity boundary eventually propagate to the cavity corners, where they can escape and give real power loss [9]. Thus, a finite cavity does not provide 100% reflectivity even for TIR states. Here this situation is analyzed further, to obtain lifetime estimates for the modes that can be approximately TIR-confined, assuming a large dielectric mismatch across the cavity boundary.

We assume two-dimensional electromagnetics (2D E&M), that is, fields that have no dependence on a longitudinal coordinate z that lies along the axis of symmetry of a prism. Analysis of the electromagnetic field boundary conditions shows that when a mode is strongly confined in the cavity by TIR, Dirichlet boundary conditions (DBC) apply approximately for both the TM and TE polarizations. This field analysis also is needed later for the boundary wave power calculations. Each mode of a triangular cavity is composed from a set of six plane waves; as such, we use a simplified analysis rather than a full solution to Maxwell's equations, such as the boundary element method [13] or finite difference time domain numerics[14]. The plane wave components of each mode are analyzed here in terms of Maxwell's equations and the related Fresnel amplitude ratios, which are slightly different for TM and TE polarizations [15]. Following Wiersig [9], it is assumed that the power radiated from a mode in the TIR regime is primarily due to the leakage of the evanescent boundary waves at the three corners of the triangle. At large index mismatch, this analysis predicts longer estimated lifetimes for the TE modes, enhanced by a factor of the order of the squared index ratio $(n/n')^2$, when compared to the lifetime of the corresponding TM mode.

2. 2D Electromagnetics at the cavity boundary

Presence of nonzero k_z for a dielectric waveguide surrounded by a different dielectric medium, in general, does not lead to separated TM and TE modes, see Ref. [15]. For 2D E&M problems (longitudinal wavevector $k_z = 0$), however, Maxwell's equations and associated boundary conditions imply independent TM and TE polarizations of the

fields. It is well-known that in a waveguide or resonator with *conducting* boundaries, the field $\psi = E_z$ for TM modes satisfies DBC, and the field $\psi = B_z$ for TE modes satisfies Neumann boundary conditions (NBC). Alternatively, if the medium is surrounded simply by a different (nonconducting) dielectric, there still are TM or TE polarizations, but, strictly speaking, these would satisfy more involved boundary conditions of Maxwell's equations, rather than the oversimplified DBC or NBC. If the fields are strongly undergoing TIR (incident angle well beyond the critical angle), however, both polarizations are shown here to satisfy DBC, in an approximate sense.

Consider a planar boundary between two media, where the boundary defines the xz -plane. The region $y < 0$, within our cavity, is occupied by a medium of index $n = \sqrt{\epsilon\mu}$, while the region $y > 0$, outside the cavity, is occupied by a medium of index $n' = \sqrt{\epsilon'\mu'}$, with $n > n'$. Primes refer to quantities on the refracted wave side (outside the cavity). The wavevector magnitudes are $k = \frac{\omega}{c}\sqrt{\epsilon\mu}$ and $k' = \frac{\omega}{c}\sqrt{\epsilon'\mu'}$ in the two media. A 2D plane wave $\sim e^{i(k_x x + k_y y)}$ with fields \vec{E}_i, \vec{B}_i , propagating in medium n with $\vec{k}_i = (k_x, k_y) = k(\sin \theta_i, \cos \theta_i)$ and incident on the boundary at angle θ_i , can be polarized either in the TM or TE polarizations (see Chap. 7 of Ref. [15]).

TM polarization: For incident $\vec{E}_i = E_i^0 \hat{z} e^{i(k_x x + k_y y)}$ perpendicular to the plane of incidence, there is also a reflected wave $\vec{E}_r = E_r^0 \hat{z} e^{i(k_x x - k_y y)}$ with the same polarization, but a different magnitude and phase, $E_r^0 = E_i^0 e^{i\alpha}$, by the Fresnel formula

$$e^{i\alpha} = \frac{\sqrt{\frac{\epsilon}{\mu}} \cos \theta_i - \sqrt{\frac{\epsilon'}{\mu'}} \cos \theta'}{\sqrt{\frac{\epsilon}{\mu}} \cos \theta_i + \sqrt{\frac{\epsilon'}{\mu'}} \cos \theta'} \quad (1)$$

Here θ' is the angle of the refracted wave, obtained from Snell's Law, $n \sin \theta_i = n' \sin \theta'$, which implies TIR when θ_i surpasses the critical angle θ_c , defined by

$$\sin \theta_c = \frac{n'}{n}. \quad (2)$$

Under TIR, E_r^0 has the same magnitude as E_i^0 , but is phase shifted by angle α , because the cosine of the refracted wave becomes pure imaginary:

$$\cos \theta' = i\gamma, \quad \gamma = \sqrt{(\sin \theta_i / \sin \theta_c)^2 - 1}. \quad (3)$$

Then it is useful to express the phase difference between the incident and reflected waves as

$$\tan \frac{\alpha}{2} = -\frac{\mu}{\mu'} \sqrt{\frac{\cos^2 \theta_c}{\cos^2 \theta_i} - 1} \quad (4)$$

The linear combination of incident and reflected waves in medium n is $\vec{E} = \vec{E}_i + \vec{E}_r = E_z \hat{z}$, having the spatial variation approaching the boundary (region $y < 0$),

$$E_z = E_i + E_r = 2E_i^0 e^{i\frac{\alpha}{2}} e^{ik_x x} \cos \left(k_y y - \frac{\alpha}{2} \right) \quad (5)$$

Corresponding to this is the associated evanescent wave in medium n' (region $y > 0$),

$$E'_z = 2E_i^0 \cos(\alpha/2) e^{i\frac{\alpha}{2}} e^{ik_x x} e^{-k'\gamma y}, \quad (6)$$

where $k_x = k'_x$ due to Snell's Law. Equation (5) shows that the E_z field on the incident side acquires a node at the boundary $y = 0$ and satisfies Dirichlet BC only when the phase shift attains the value $\alpha = -\pi$. According to Equation (4), this occurs only in the limit $\theta_i \rightarrow 90^\circ$, i.e., extreme grazing incidence. Alternatively, at the *threshold* for TIR ($\theta = \theta_c$), Equation (4) gives $\alpha = 0$, whereby (5) indicates that the E_z field now will peak at $y = 0$ and satisfies a Neumann BC.

Seeing that the BC on E_z ranges between the two extremes of DBC and NBC, clearly neither boundary condition is fully applicable to the TIR regime. However, it suggests that one should use NBC for finding the TIR threshold conditions, and DBC to determine the field distributions at large enough index mismatch. One can get some indication of the crossover to DBC-like behavior by locating the incident angle $\theta_i = \tilde{\theta}$ where the phase shift passes $\frac{-\pi}{2}$, i.e., when $\tan \frac{\alpha}{2} = -1$. From Equation (4) one finds

$$\cos \tilde{\theta} = \frac{\cos \theta_c}{\sqrt{1 + \left(\frac{\mu'}{\mu}\right)^2}}. \quad (7)$$

In the usual practical situation, with $\mu = \mu' \approx 1$, we have $\cos \tilde{\theta} = \frac{1}{\sqrt{2}} \cos \theta_c$. For usual optical media with very weak magnetic properties, one sees that a large index ratio $n/n' \approx \sqrt{\epsilon/\epsilon'}$ does not increase the range of applicability of Dirichlet BC for TM polarization. To give a numerical example, for a weak index mismatch with $\sin \theta_c = 1/2$, giving $\theta_c = 30^\circ$, the crossover angle is $\tilde{\theta} = 52.2^\circ$; in order to reach phase angle $\alpha = -0.9\pi$, quite close to DBC, requires an incident angle $\theta_i = 82.2^\circ$. Even for a larger mismatch $\sin \theta_c = 1/4$, with $\theta_c = 14.5^\circ$, one gets only a slight improvement to $\tilde{\theta} = 46.8^\circ$, and to get to $\alpha = -0.9\pi$ still requires $\theta_i = 81.3^\circ$.

We see that it makes some sense to apply NBC to find the limiting conditions for TIR of a single plane wave, but, in general, provided the incident angle is sufficiently larger than the crossover angle $\tilde{\theta}$, the fields on the incident side (within the cavity) approximately satisfy DBC. The adequacy of DBC improves with higher index mismatch, but not as strongly as one would hope, because the phase angle does not depend on the dielectric permittivities for TM polarization.

TE polarization: Now the magnetic field \vec{B} is polarized in the \hat{z} direction everywhere, and controls the other fields, according to relations $\vec{B} = \sqrt{\epsilon\mu} \hat{k} \times \vec{E}$ for each plane wave, and amplitude relations $B = \sqrt{\epsilon\mu} E$. Taking incident wave $\vec{B}_i = B_i^0 \hat{z} e^{i(k_x x + k_y y)}$, with electric field amplitude $E_i^0 = B_i^0 / \sqrt{\epsilon\mu}$, there is a reflected wave $\vec{B}_r = B_r^0 \hat{z} e^{i(k_x x - k_y y)}$, with electric field amplitude $E_r^0 = B_r^0 / \sqrt{\epsilon\mu}$. The amplitude ratio $E_r^0/E_i^0 = e^{i\alpha}$ is described by the Fresnel formula:

$$e^{i\alpha} = \frac{\sqrt{\frac{\epsilon'}{\mu'}} \cos \theta_i - \sqrt{\frac{\epsilon}{\mu}} \cos \theta'}{\sqrt{\frac{\epsilon'}{\mu'}} \cos \theta_i + \sqrt{\frac{\epsilon}{\mu}} \cos \theta'} \quad (8)$$

The phase difference between the incident and reflected waves can be expressed as

$$\tan \frac{\alpha}{2} = -\frac{\epsilon}{\epsilon'} \sqrt{\frac{\cos^2 \theta_c}{\cos^2 \theta_i} - 1}. \quad (9)$$

The linear combination of incident and reflected magnetic waves in medium \mathbf{n} is $\vec{B} = \vec{B}_i + \vec{B}_r = B_z \hat{z}$, and mirrors the behavior of \vec{E} for the TM problem, having the spatial variation approaching the boundary,

$$B_z = B_i + B_r = 2B_i^0 e^{i\frac{\alpha}{2}} e^{ik_x x} \cos\left(k_y y - \frac{\alpha}{2}\right) \quad (10)$$

The associated evanescent wave in medium \mathbf{n}' is

$$B'_z = 2B_i^0 \cos(\alpha/2) e^{i\frac{\alpha}{2}} e^{ik_x x} e^{-k' \gamma y}. \quad (11)$$

The behavior of B_z near the boundary for TE polarization is the same as that for E_z near the boundary for TM polarization. It means that provided the incident angle is far enough beyond the critical angle, one could also apply DBC for TE fields; NBC would only be reasonable just beyond the TIR threshold, for a single plane wave. However, due to the presence of the permittivity ratio in Equation (9), a large index mismatch enhances the applicability of DBC for TE polarization. The crossover incident angle $\tilde{\theta}$ at which $\tan \frac{\alpha}{2} = -1$ is now

$$\cos \tilde{\theta} = \frac{\cos \theta_c}{\sqrt{1 + \left(\frac{\epsilon'}{\epsilon}\right)^2}} \approx \frac{\cos \theta_c}{\sqrt{1 + \left(\frac{n'}{n}\right)^4}}, \quad (12)$$

where the latter expression applies when $\mu \approx \mu'$. Now the modest index mismatch with $\sin \theta_c = 1/2$ and $\theta_c = 30^\circ$ leads to a very nearby crossover angle $\tilde{\theta} = 32.8^\circ$, meaning that the strong TIR regime and region of adequate applicability of DBC is very wide. For larger mismatch $\sin \theta_c = 1/4$ with $\theta_c = 14.5^\circ$, the DBC regime is even closer to θ_c , beginning around $\tilde{\theta} = 14.9^\circ$. Thus, application of DBC for the modes of a cavity with TE field polarization should be very acceptable, even more so than for TM polarization, except when the mode is extremely close to the TIR threshold.

Within mentioned limitations, we continue discussing the modes in a 2D equilateral triangle of edge length a , under the assumption of DBC for both polarizations.

3. Exact modes for an equilateral triangle with DBC

The triangular cross section in physical problems has evoked interest ever since the first solution for triangular elastic membranes by Lamé [16]. Related problems have been solved analytically [17, 18, 19] for both DBC and Neumann BC, including quantum billiards [20, 21, 22, 23], quantum dots [24], and lasing modes in resonators and mirrored dielectric cavities [2, 25].

Coordinates are used with the origin at the geometrical center of the triangle of edge length a , and the lower edge parallel to the x -axis, as in Fig. 1. The notation b_0 , b_1 , and b_2 is used to denote the lower, upper right, and upper left boundaries, respectively.

The general solution is a superposition of six plane waves, obtained by 120-degree rotations of one partially standing wave ψ_0 , which goes to zero on boundary b_0 , with $\vec{k}_1 = k_1 \hat{x}$ and $\vec{k}_2 = k_2 \hat{y} \neq 0$:

$$\psi_0 = e^{i\vec{k}_1 \cdot \vec{r}} \sin \left[\vec{k}_2 \cdot \vec{r} + \frac{k_2 a}{2\sqrt{3}} \right] \quad (13)$$

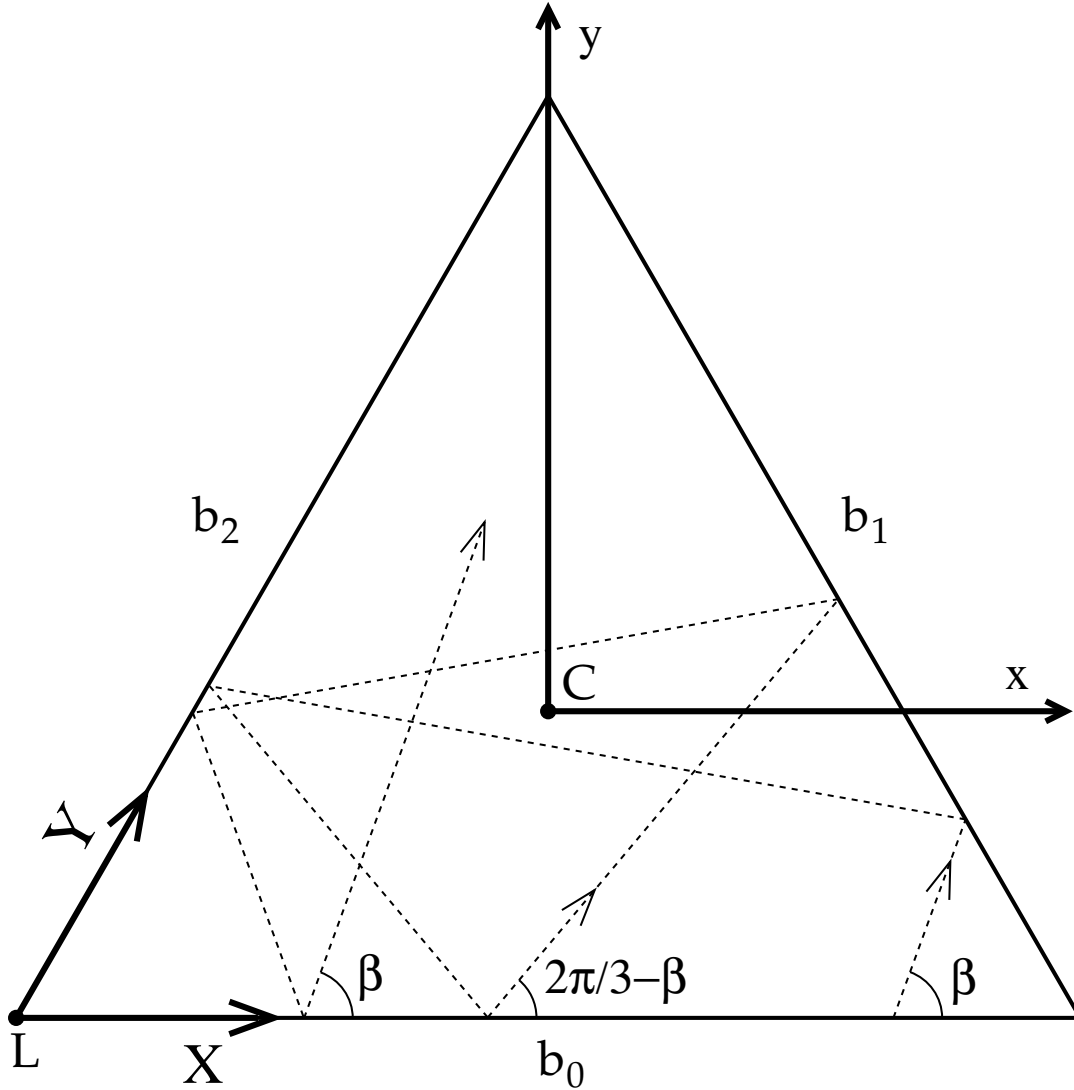


Figure 1. Coordinates for a 2D triangular cavity of edge a . The geometrical center at C , the origin of the xy -coordinates, is a distance $\frac{a}{2\sqrt{3}}$ above the lower (b_0) edge. The lower left corner L is the origin of the skew XY -coordinates. The dashed line demonstrates the reflections of a ray originating at angle $\beta = 70^\circ$ to the lower edge, requiring two complete circuits to return to the same angle.

Rotations of ψ_0 through 120° and 240° produce related wavefunctions ψ_1 and ψ_2 which go to zero on b_1 and b_2 , respectively. The net wavefunction can be written as

$$\psi = \mathcal{A}_0\psi_0 + \mathcal{A}_1\psi_1 + \mathcal{A}_2\psi_2, \quad (14)$$

where the relative phases of the components are

$$\mathcal{A}_1 = \mathcal{A}_0 e^{i\frac{2\pi}{3}m}, \quad \mathcal{A}_2 = \mathcal{A}_0 e^{-i\frac{2\pi}{3}m}. \quad (15)$$

and the allowed wavevectors are

$$k_1 = \frac{2\pi}{3a}m, \quad m = 0, 1, 2, \dots \quad (16)$$

$$k_2 = \frac{2\pi}{3a} \sqrt{3} n. \quad n = 1, 2, 3, \dots \quad (17)$$

Indexes n and m must be of the same parity with $m < n$. The resulting frequencies are

$$\omega = c^* \sqrt{k_1^2 + k_2^2} = \frac{c}{\sqrt{\epsilon\mu}} \frac{2\pi}{3a} \sqrt{m^2 + 3n^2} \quad (18)$$

where $c^* = c/\sqrt{\epsilon\mu}$ is the speed of light in the cavity. This physically motivated form for ψ was described by Chang *et al.* [2] and is equivalent to the first solution given by Lamé' [16] and used by many authors [19]. Wavefunctions for the sequence of many of the lowest modes are displayed at www.phys.ksu.edu/~wysin/. Only those with $m \neq 0$ can be confined by TIR. Based on a straightforward analysis of the six plane wave components, using Snell's Law and requiring all incident angles greater than the critical angle, the index ratio required for confinement by TIR can be shown to be

$$\frac{n}{n'} > N_c = \sqrt{3 \frac{n^2}{m^2} + 1}. \quad (19)$$

4. TIR mode lifetimes

When all of the plane wave components in ψ satisfy the TIR conditions, there is still the possibility for the cavity fields to decay in time. Clearly, we have only an approximate solution, since DBC is not exactly the correct boundary condition. The effect this causes is difficult to estimate. Another source of decay are diffractive effects: the finite length of the triangle edge and the presence of sharp corners is likely to have special influence on the TIR that is difficult to predict. One feature, however, which can be considered as due to diffraction, is the leakage of *boundary waves* at the corners of the triangle [9]. Under conditions of TIR, an evanescent wave exists within the exterior medium, decaying exponentially into that medium, and moving parallel to the cavity surface. When it encounters the corner of that edge, a sharp discontinuity in the surface, it can be expected to constitute power radiated from the cavity. Here we consider the mode lifetime estimates based solely on the losses due to these boundary waves.

Based on the ratio of the total energy U stored in the cavity fields, compared to the total power P emitted by the boundary waves from all the corners, an upper limit of the mode lifetime can be estimated as

$$\tau = \frac{U}{P}. \quad (20)$$

The calculations of U and P have slight differences for TM versus TE polarization. Therefore, there is no reason to expect these lifetimes to be the same.

Cavity energy: For both polarizations, we use the wavefunction ψ reviewed in Sec. 3, which can be expressed as

$$\begin{aligned} \psi = \mathcal{A}_0 \left\{ e^{ik_1 x} \sin \left[k_2 \left(y + \frac{a}{2\sqrt{3}} \right) \right] \right. \\ \left. + e^{ik_1 \left(-\frac{1}{2}x + \frac{\sqrt{3}}{2}y + a \right)} \sin \left[k_2 \left(-\frac{\sqrt{3}}{2}x - \frac{1}{2}y + \frac{a}{2\sqrt{3}} \right) \right] \right\} \end{aligned} \quad (21)$$

$$+ e^{ik_1(-\frac{1}{2}x - \frac{\sqrt{3}}{2}y - a)} \sin \left[k_2 \left(\frac{\sqrt{3}}{2}x - \frac{1}{2}y + \frac{a}{2\sqrt{3}} \right) \right] \Big\}$$

The total energy of the fields within the cavity of height h can be written as

$$U = \int h \, dx \, dy \frac{\epsilon |\vec{E}|^2}{8\pi} = \int h \, dx \, dy \frac{|\vec{B}|^2}{8\pi\mu}; \quad (22)$$

the first form is convenient for TM modes ($|\vec{E}|^2 = |\psi|^2$), the second is convenient for TE modes ($|\vec{B}|^2 = |\psi|^2$). So both calculations require the normalization integral of ψ . This integral can be simplified by a transformation to a skew coordinate system whose axes are aligned to two edges of the triangle, as shown in Fig. 1. Placing the origin of the new coordinates (X, Y) at the lower left corner of the triangle, with X increasing from 0 to a along edge b_0 , and Y increasing from 0 to a along edge b_2 , we have

$$\begin{aligned} X + Y \cos 60^\circ &= x + \frac{a}{2}, \\ Y \sin 60^\circ &= y + \frac{a}{2\sqrt{3}}. \end{aligned} \quad (23)$$

The numbers $(\frac{a}{2}, \frac{a}{2\sqrt{3}})$ are simply the displacement of the origin (vector from triangle corner L to center C). The wavefunction is now expressed as

$$\begin{aligned} \psi &= \mathcal{A}_0 \left\{ e^{ik_1(X + \frac{1}{2}Y - \frac{a}{2})} \sin \left[\frac{\sqrt{3}}{2} k_2 Y \right] \right. \\ &\quad + e^{ik_1(-\frac{1}{2}X + \frac{1}{2}Y + a)} \sin \left[\frac{\sqrt{3}}{2} k_2 (-X - Y + a) \right] \\ &\quad \left. + e^{ik_1(-\frac{1}{2}X - Y - \frac{a}{2})} \sin \left[\frac{\sqrt{3}}{2} k_2 X \right] \right\}. \end{aligned} \quad (24)$$

In this form, it is more obvious that each term goes to zero on one of the boundaries, $X = 0$ (b_2), $Y = 0$ (b_0), or $X + Y = a$ (b_1). Using the periodicity of ψ , the integration over the triangular area is effected by

$$\int dx \, dy = \frac{1}{2} \int_0^a dX \int_0^a dY |J| \quad (25)$$

where the Jacobian is $|J| = \frac{\sqrt{3}}{2}$ and the factor of $\frac{1}{2}$ cancels integrating over two triangles. The absolute square of ψ involves three direct terms (squared sines involving only k_2) and six cross terms from Equation (24). It is possible to show that the cross terms integrated over the triangular area all are zero, due to the special choices of allowed k_1 and k_2 given by (16) and (17). The remaining nonzero parts result in

$$\int dx \, dy |\psi|^2 = \frac{3\sqrt{3}}{8} a^2 |\mathcal{A}_0|^2. \quad (26)$$

Boundary wave power: The symmetry of the wavefunction causes the boundary wave power out of each edge to be the same, therefore, we calculate that occurring in edge b_0 (at $y = 0$) and multiply by three for the total power. This calculation follows that presented by Wiersig [9] for resonant fields in a regular polygon.

Looking at the wavefunction (21), one can see that there are three distinct plane waves *incident* on b_0 . First is the wave with the smallest angle of incidence, resulting from the first term in (21),

$$\psi_0^- = \frac{-\mathcal{A}_0}{2i} e^{\frac{-ik_2 a}{2\sqrt{3}}} e^{i(k_1 x - k_2 y)}. \quad (27)$$

Using the allowed values for k_1 and k_2 , the angle of incidence is seen to be

$$\sin \theta_0^- = \frac{m}{\sqrt{m^2 + 3n^2}}. \quad (28)$$

Next, there is a wave with the largest magnitude incident angle, due to the second term in (21),

$$\psi_1^+ = \frac{\mathcal{A}_0}{2i} e^{i(k_1 + \frac{k_2}{2\sqrt{3}})a} e^{i[(-\frac{1}{2}k_1 - \frac{\sqrt{3}}{2}k_2)x + (\frac{\sqrt{3}}{2}k_1 - \frac{1}{2}k_2)y]}, \quad (29)$$

whose incident angle is

$$\sin \theta_1^+ = \frac{1}{2} \frac{-m - 3n}{\sqrt{m^2 + 3n^2}}. \quad (30)$$

A negative value of θ_{1+} means the wave is propagating contrary to the x -axis. Finally, the last term in (21) leads to a wave with an intermediate incident angle,

$$\psi_2^+ = \frac{\mathcal{A}_0}{2i} e^{i(-k_1 + \frac{k_2}{2\sqrt{3}})a} e^{i[(-\frac{1}{2}k_1 + \frac{\sqrt{3}}{2}k_2)x + (-\frac{\sqrt{3}}{2}k_1 - \frac{1}{2}k_2)y]}, \quad (31)$$

whose incident angle is

$$\sin \theta_2^+ = \frac{1}{2} \frac{-m + 3n}{\sqrt{m^2 + 3n^2}}. \quad (32)$$

The plus/minus superscripts on these waves refer to the positive/negative exponents in the sine functions of Equation (21).

Now, for each of these incident waves, there is a corresponding evanescent wave propagating along the edge of the cavity; these are assumed to produce emitted power when encountering the triangle corners. The Poynting vector \vec{S}' associated with a single plane evanescent wave along the b_0 boundary is

$$\vec{S}' = \frac{c}{8\pi} \Re(\vec{E}' \times \vec{H}'^*) = \frac{c}{8\pi} \sqrt{\frac{\epsilon'}{\mu'}} |\vec{E}'|^2 \sin \theta' \hat{x} \quad (33)$$

On the other hand, the linear superposition of the three waves $\psi_0^-, \psi_1^+, \psi_2^+$ leads to an interference pattern both within the cavity, and in the evanescent waves and exterior power flow. Careful consideration of a linear combination of two waves shows that, although interference leads to a spatially varying \vec{S}' with components both parallel and perpendicular to the boundary, an integral number of wavelengths of that pattern fits along the edge. Thus, it is clear that the interference effects can be ignored in the calculation of the emitted boundary power. For the total emitted power due to boundary waves, it is sufficient to sum the individual powers for the three independent incident waves.

For **TM polarization**, with $\psi = E_z$, the exterior electric field of a single evanescent wave has only a z -component like that in Equation (6). Applying Snell's law, and

integrating the Poynting vector from $y = 0$ to $y = \infty$, the power flow along \hat{x} in one boundary wave, on one edge, is

$$P_x = \frac{ch}{4\pi\mu'} \frac{|E_i^0|^2}{\omega/c} \frac{n \sin \theta_i}{\sqrt{(n \sin \theta_i)^2 - (n')^2}} \cos^2 \frac{\alpha}{2} \quad (34)$$

where α is the phase shift given by (4) in Sec. 2. One can see that the boundary wave power has a dependence on $(\sin \theta_i - \sin \theta_c)^{-1/2}$. Although each of the waves $\psi_0^-, \psi_1^+, \psi_2^+$ will produce a boundary wave emission, the wave ψ_0^- has the smallest angle of incidence, and produces by far the largest boundary wave power. This can be seen by examining the expressions for incident angles θ_0^-, θ_1^+ and θ_2^+ , and using the facts that $m < n$ and m, n have the same parity. Therefore a good lifetime estimate can be made using only the power due to ψ_0^- . From the expression (27) for ψ_0^- , the squared magnitude of its electric field is $|E_i^0|^2 = \frac{1}{4} |\mathcal{A}_0|^2$. From expressions (26) and (22), the total TM cavity energy is

$$U_{\text{TM}} = \frac{\epsilon h}{8\pi} \frac{3\sqrt{3}}{8} a^2 |\mathcal{A}_0|^2. \quad (35)$$

The estimate of the lifetime due to boundary wave emission only, from all three edges combined, is $\tau_{\text{TM}} \approx U_{\text{TM}}/3P_x$. It is convenient to express the result in dimensionless form, scaling with the mode frequency to give the quality factor Q_{TM} ,

$$Q_{\text{TM}} = \omega \tau_{\text{TM}} \approx \frac{\sqrt{3}}{4} \left(\frac{\omega a}{c^*} \right)^2 \frac{\sqrt{1 - (\sin \theta_c / \sin \theta_0^-)^2}}{\cos^2 \theta_0^-} \times \frac{\mu}{\mu'} \left[\sin^2 \theta_0^- - \sin^2 \theta_c + \left(\frac{\mu'}{\mu} \right)^2 \cos^2 \theta_0^- \right], \quad (36)$$

where θ_0^- depends on the mode quantum numbers according to Equation (28). In the usual case where $\mu \approx \mu'$, the second line of the formula simplifies to just $\cos^2 \theta_c$.

Obviously, when θ_0^- approaches θ_c , which would occur at weak enough index mismatch, the estimated lifetime $\tau_{\text{TM}} \rightarrow 0$, which is the limit of a non-bound state. At the opposite extreme of large index mismatch where $n/n' \gg 1$, this estimate varies as $1/\cos^2 \theta_0^-$, and since $\omega a/c^*$ is a number of order unity, the order of magnitude is determined by

$$\tau_{\text{TM}} \sim \frac{a}{c} \sqrt{\epsilon \mu}. \quad (37)$$

The result is interesting because it shows a lifetime that increases with the triangle size, as well as being proportional to the refractive index in the cavity.

For **TE polarization**, with $\psi = B_z$, the exterior magnetic field of a single evanescent wave has only a z -component like that in Equation (11). The calculation follows the same reasoning as used for the TM modes, but the specific details lead to a slightly different result. Definition of the Poynting vector as in Equation (33) is the same. The substitution $|\vec{E}'| = |B'_z|/\sqrt{\epsilon'\mu'}$ together with Equation (11) for B'_z , followed

by $|E_i^0| = |B_i^0|/\sqrt{\epsilon\mu}$ within the cavity, leads to the boundary wave power with extra factors,

$$P_x = \frac{ch}{4\pi\mu'} \frac{\mu'\epsilon}{\epsilon'\mu} \frac{|E_i^0|^2}{\omega/c} \frac{n \sin \theta_i}{\sqrt{(n \sin \theta_i)^2 - (n')^2}} \cos^2 \frac{\alpha}{2} \quad (38)$$

where now the phase shift α given by (9) in Sec. 2 depends on the ratio $\epsilon/\epsilon' \gg 1$ rather than $\mu/\mu' \approx 1$. Furthermore, using (26) and (22), the energy stored in the cavity fields is now

$$U_{\text{TE}} = \frac{h}{8\pi\mu} \frac{3\sqrt{3}}{8} a^2 |\mathcal{A}_0|^2. \quad (39)$$

With cavity magnetic field strength $|B_i^0|^2 = \frac{1}{4} |\mathcal{A}_0|^2$, and again estimating the lifetime using only the ψ_0^- boundary wave from all three edges, the lifetime is $\tau_{\text{TE}} \approx U_{\text{TE}}/3P_x$. One finds the quality factor,

$$Q_{\text{TE}} = \omega\tau_{\text{TE}} \approx \frac{\sqrt{3}}{4} \left(\frac{\omega a}{c^*} \right)^2 \frac{\sqrt{1 - (\sin \theta_c / \sin \theta_0^-)^2}}{\cos^2 \theta_0^-} \times \frac{\epsilon}{\epsilon'} \left[\sin^2 \theta_0^- - \sin^2 \theta_c + \left(\frac{\epsilon'}{\epsilon} \right)^2 \cos^2 \theta_0^- \right]. \quad (40)$$

The second line of this formula highlights the difference for TE polarization compared to TM. The factor in the brackets is some number less than 1; it contrasts the bracket which reduces to $\cos^2 \theta_c$ in formula (36) for the TM polarization lifetime when $\mu = \mu'$. The crucial difference is the factor $\epsilon/\epsilon' \gg 1$ present here, compared to a similar factor $\mu'/\mu \approx 1$ for the TM lifetime formula. This is the more dominant factor, and it suggests that roughly speaking, the ratio of the lifetimes for the two polarizations, which have the same (approximately DBC) boundary conditions and frequencies, is

$$\frac{\tau_{\text{TE}}}{\tau_{\text{TM}}} \approx \frac{\epsilon}{\epsilon'} = \left(\frac{n}{n'} \right)^2. \quad (41)$$

The result holds as long as the index mismatch is adequately large compared to the cutoff value needed to stabilize that mode by TIR. Otherwise, at smaller index mismatch, the TM lifetime can be longer than the TE lifetime.

Some results for τ_{TM} are presented in Fig. 2, showing lifetimes as functions of the index mismatch for some of the lowest modes. Scaled by the triangle size and light speed in the cavity, the lifetimes increase abruptly above the TIR confinement limits, eventually increasing at a slower rate. For the modes shown, dimensionless frequencies $\omega a/c^*$ are typically numbers greater than 10 [See Equation (18)], with the values of $\tau c^*/a$ also of the order of 10. Combining these rough results, the mode lifetimes in units of the mode periods T are similar to

$$\frac{\tau}{T} = \frac{\omega\tau}{2\pi} \sim \frac{10 \times 10}{2\pi} \approx 16. \quad (42)$$

Assuming that the lifetime estimates have included the dominant loss mechanism in the cavity, this result for τ/T indicates that the original assumption of a resonance mode weakly confined by TIR should be a valid concept. Obviously, this holds far enough

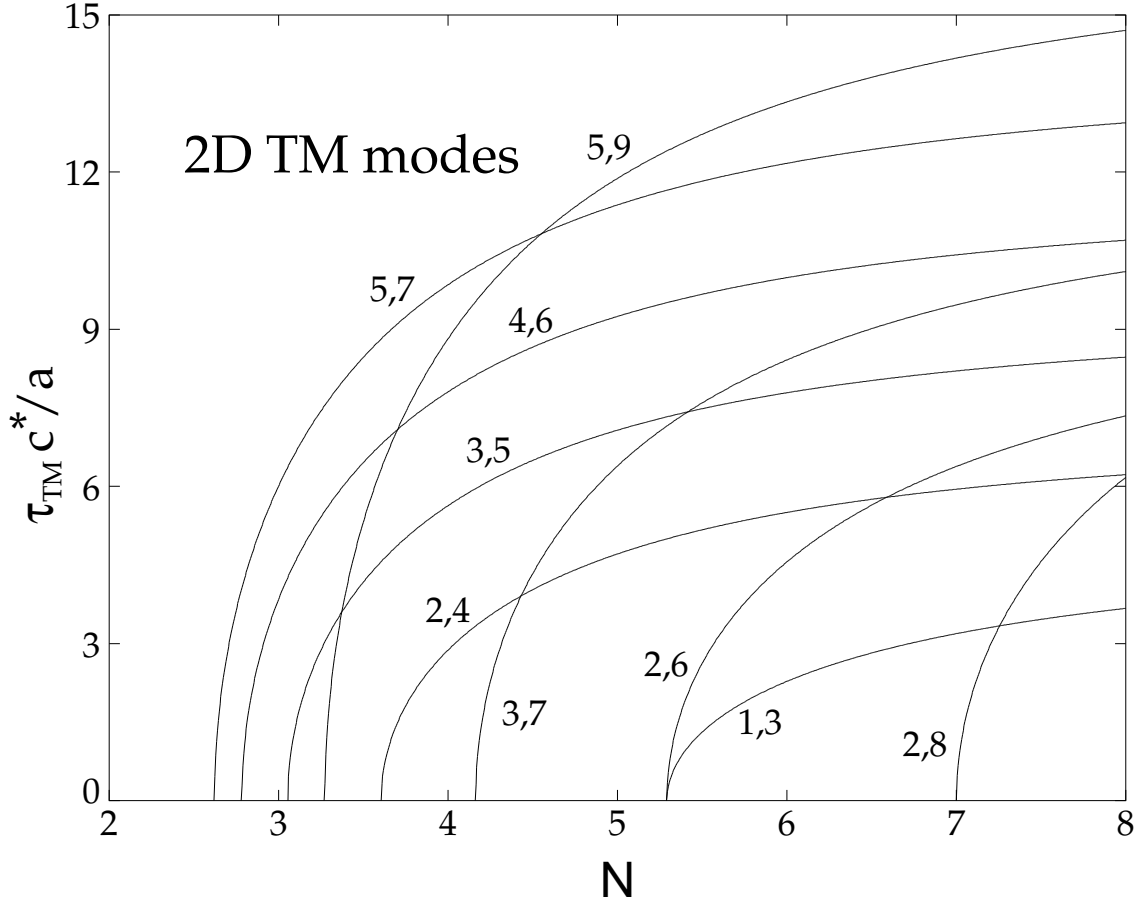


Figure 2. Estimated lifetimes for some low TM modes indicated by (m, n) pairs, versus the index ratio $N = \frac{n}{m}$. The lifetime is scaled by a/c^* , the signal propagation time across the cavity, where c^* is the speed of light in the cavity medium.

above the TIR confinement limits only, keeping in mind the approximate nature of the Dirichlet boundary conditions that were applied.

Comparative results for τ_{TE} for the same mode indexes are shown in Fig. 3. Due to the presence of the extra factor of $\epsilon/\epsilon' \approx N^2$, these lifetimes increase more rapidly than the TM lifetimes. As an example, for mode $(3, 5)$, the TE lifetime is about 6 times longer than the TM lifetime at $N = 8$. On the other hand, for the mode $(1, 3)$, which has a much larger TIR confinement limit, the TE lifetime is only about 1/3 longer than the TM lifetime at $N = 8$. Clearly, modes with (m, n) indexes nearly the same, as in the form $(m, m+2)$ with large m , require smaller index mismatch for TIR confinement, and will more closely follow the lifetime ratio determined strongly by the index mismatch, Equation (41).

In earlier experiments [2] triangular semiconductor cavities with edges ranging from 75 to 350 μm were used. Assuming an effective index of refraction around $n \approx 4$, with vacuum on the exterior, and using $a \approx 100\mu\text{m}$, (37) and (41) give rough lower estimates $\tau_{TM} \sim 1.3$ ps, and $\tau_{TE} \sim 20$ ps. Of course, for practical purposes of maintaining

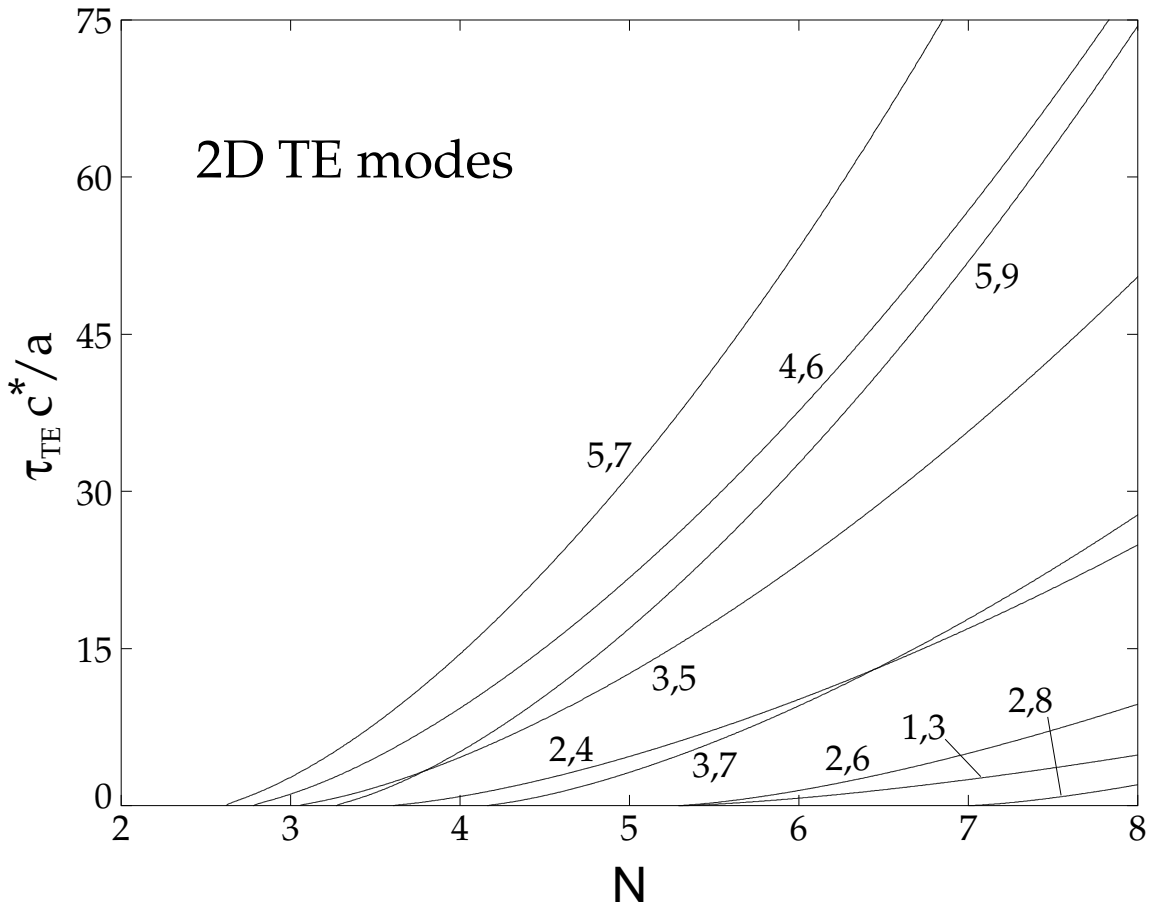


Figure 3. Estimated lifetimes for low TE modes indicated by (m, n) pairs, versus the index ratio $N = \frac{n}{m}$. These lifetimes are larger than the corresponding TM lifetimes (Fig. 2) when N is sufficiently larger than the cutoff value for that mode.

a resonating mode, a large value of τ/T is much more relevant, as discussed above. Based on these calculations, smaller cavities will have reduced lifetimes, but also shorter oscillation periods in the same ratio. For large index ratio, where $\sin \theta_c \ll 1$, $\cos \theta_c \approx 1$, and using the fact that $m < n$, lifetime expression (36) and frequency expression (18) produce the estimate,

$$\frac{\tau_{\text{TM}}}{T} \approx \frac{\pi^2 n^2}{\sqrt{3}}. \quad (43)$$

This ratio is independent of the cavity size or dielectric properties, increasing only with the squared mode quantum number n . For example, at index ratio $N = 4$, Equation (19) shows that the lowest TIR-confined mode has $(m, n) = (2, 4)$. Then an estimate of its quality factor, based on Equation (43), is $Q_{\text{TM}} = 2\pi\tau_{\text{TM}}/T \approx 500$, somewhat larger than recent experimental results on $5 - 20 \mu\text{m}$ cavities [3], but similar to or smaller than other theoretical analysis[11]. The TE mode lifetime (and Q) under these assumptions should be even larger, by the squared refractive index ratio $(n/n')^2$. Of course, these should be considered over-estimates for Q , as only the losses due to boundary waves

have been included.

5. Conclusions

The resonant mode lifetimes of an optical cavity with an equilateral triangular cross-section have been estimated approximately, employing the exact analytic triangle solutions for Dirichlet boundary conditions. Deep enough in the TIR regime, both TE and TM polarizations can be adequately described using DBC. (Neumann BC applies to either polarization of a single plane wave exactly at the TIR threshold.) Furthermore, the transition into the TIR regime is much sharper for TE polarization than for TM polarization. An increased index mismatch at the cavity boundary aids the confinement of the TE polarization much more than the TM polarization. This means that for the plane wave components with incident angles only slightly above the critical value, the DBC approximation is typically much better for TE polarization than for TM polarization.

The different polarization-dependent Fresnel factors associated with the cavity boundary produce different rates of energy loss due to evanescent boundary waves. For these 2D E&M fields at large index mismatch between the cavity and its exterior, this leads to considerably longer lifetimes for TE polarization, enhanced approximately by a factor of the squared index ratio $(n/n')^2$ compared to the TM lifetime. Conversely, the differences in these lifetimes would be expected to imply stronger coupling of EM fields from outside to inside the cavity in the TM polarization. This suggests that stimulation and generation of the modes by an external light source should be more efficient for TM polarization.

Acknowledgments

The author acknowledges helpful discussions with A. R. Pereira at the Universidade Federal de Viçosa, Brazil, where this work was completed with support from FAPEMIG.

References

- [1] McCall S L, Levi A F J, Slusher R E, Pearton S J and Logan R A 1992 Whispering gallery modes in microdisk lasers *Appl. Phys. Lett.* **60** 289
- [2] Chang H C, Kioseoglou G, Lee E H, Haetty J, Na M H, Xuan Y, Luo H, Petrou A and Cartwright A N 2000 Lasing modes in equilateral-triangular laser cavities *Phys. Rev. A* **62** 013816
- [3] Lu Q Y, Chen X H, Guo W H, Yu L J, Huang Y Z, Wang J, Luo Y 2004 Mode characteristics of semiconductor equilateral triangle microcavities with side length of 5–20 μm *IEEE Photon. Technol. Lett.* **16** 359
- [4] Poon A W, Courvoisier F and Chang R K 2001 Multimode resonances in square-shaped optical microcavities *Opt. Lett.* **26** 632
- [5] Fong C Y and Poon A W 2003 Mode field patterns and preferential mode coupling in planar waveguide-coupled square microcavities *Optics Express* **11**, 2897
- [6] Moon H-J, An K and Lee J-H 2003 Single spatial mode selection in a layered square microcavity laser *Appl. Phys. Lett.* **82**, 2963

- [7] Vietze U *et al.* 1998 Zeolite-dye microlasers. *Phys. Rev. Lett.* **81** 4628
- [8] Braun I *et al.* 2000 Hexagonal microlasers based on organic dyes in nanoporous crystals *Appl. Phys. B* **70** 335
- [9] Wiersig J 2003 Hexagonal dielectric resonators and microcrystal lasers. *Phys. Rev. A* **67** 023807
- [10] Huang Y Z 1999 Eigenmode confinement in semiconductor microcavity lasers with an equilateral triangle resonator *Proc. SPIE* **3899** 239
- [11] Guo W H, Huang Y Z and Wang Q M 2000 Resonant frequencies and quality factors for optical equilateral triangle resonators calculated by FDTD technique and the Padé approximation *IEEE Photon. Technol. Lett.* **12** 813
- [12] Huang Y Z, Guo W H and Wang Q M 2001 Analysis and numerical simulation of eigenmode characteristics for semiconductor lasers with an equilateral triangle micro-resonator *IEEE J. Quantum Electron.* **37** 100
- [13] Wiersig J 2003 Boundary element method for resonances in dielectric microcavities *J. Opt. A: Pure Appl. Opt.* **5** 53
- [14] Dey S and Mittra R 1998 Efficient computation of resonant frequencies and quality factors via a combination of the finite-difference time-domain technique and the Padé approximation *IEEE Microwave and Guided Wave Lett.* **8** 415
- [15] Jackson J D 1975 *Classical Electrodynamics* 2nd ed (John Wiley and Sons, New York 1975) Chaps. 7-8
- [16] Lamé M G 1852 *Leçons sur la théorie mathématique de l'élasticité des corps solides* (Bachelier, Paris) **57** p 131
- [17] Krishnamurthy H R, Mani H S and Verma H C 1982 Exact solution of the Schrodinger equation for a particle in a tetrahedral box *J. Phys. A: Math. Gen.* **15** 2131
- [18] Itzykson C and Luck J M 1986 Arithmetical degeneracies in simple quantum systems *J. Phys. A: Math. Gen.* **19** 211
- [19] Brack M and Bhaduri R K 1997 *Semiclassical Physics* (Addison-Wesley Frontiers in Physics) p 128
- [20] de Sales J A and Florencio J 2003 Quantum chaotic trajectories in integrable right triangular billiards *Phys. Rev. E* **67** 016216
- [21] Gutkin E 1986 Billiards in polygons *Physica* **19D** 311
- [22] Liboff R L 1994 The polygon quantum billiard problem *J. Math. Phys.* **35** 596
- [23] Molinari L 1997 On the ground state of regular polygonal billiards *J. Phys. A: Math. Gen.* **30** 6517
- [24] Brack M, Blaschke J, Creagh S C, Magner A G, Meier P and Reimann S M 1997 On the role of classical orbits in mesoscopic electronic systems *Z. Phys. D* **40** 276
- [25] Frank O and Eckhardt B 1996 Eigenvalue density oscillations in separable microwave resonators *Phys. Rev. E* **53** 4166